c-Ret–mediated hearing loss in mice with Hirschsprung disease

Nobutaka Ohgami[a], Michiru Ida-Eto[a], Takashi Shimotake[b], Naomi Sakashita[c], Michihiko Sone[d], Tsutomu Nakashima[d], Keiji Tabuchi[e], Tomofumi Hoshino[e], Atsuyoshi Shimada[f], Toyonori Tsuzuki[g], Masahiko Yamamoto[h], Gen Sobue[i], Mayumi Jijiwa[j], Naoya Asai[j], Akira Hara[e], Masahide Takahashi[j], and Masashi Kato[a,1]

[a]Unit of Environmental Health Sciences, Department of Biomedical Sciences, College of Life and Health Sciences, Chubu University, 1200 Matsumoto, Kasugai, Aichi 487-8501, Japan; [b]Department of Pediatric Surgery, Ishikawa Prefectural Central Hospital, Kanazawa, 920-8530, Japan; [c]Department of Pathology, Kumamoto University School of Medicine, Kumamoto, 860-8556, Japan; Departments of [d]Otorhinolaryngology, [i]Neurology, and [j]Pathology, Nagoya University Graduate School of Medicine, Nagoya, 466-8550, Japan; [e]Department of Otolaryngology, Institute of Clinical Medicine, University of Tsukuba, Tsukuba, 305-8575, Japan; [f]Department of Pathology, Institute for Developmental Research, Aichi Human Service Center, Aichi, 480-0392, Japan; [g]Department of Pathology, Nagoya Daini Red Cross Hospital, Nagoya, 466-8650, Japan; and [h]Department of Speech Pathology and Audiology, Aichi Gakuin University School of Health Science, Nisshin, Aichi, 470-0195, Japan

Edited by Jonathan G. Seidman, Harvard Medical School, Boston, MA, and approved June 3, 2010 (received for review April 3, 2010)

A significantly increased risk for dominant sensorineural deafness in patients who have Hirschsprung disease (HSCR) caused by *endothelin receptor type B* and *SOX10* has been reported. Despite the fact that c-*RET* is the most frequent causal gene of HSCR, it has not been determined whether impairments of c-*Ret* and c-*RET* cause congenital deafness in mice and humans. Here, we show that impaired phosphorylation of c-Ret at tyrosine 1062 causes HSCR-linked syndromic congenital deafness in c-*Ret* knockin (KI) mice. The deafness involves neurodegeneration of spiral ganglion neurons (SGNs) with not only impaired phosphorylation of Akt and NF-κB but decreased expression of calbindin D28k in inner ears. The congenital deafness involving neurodegeneration of SGNs in c-*Ret* KI mice was rescued by introducing constitutively activated RET. Taken together with our results for three patients with congenital deafness with c-*RET*–mediated severe HSCR, our results indicate that c-*Ret* and c-*RET* are a deafness-related molecule in mice and humans.

spiral ganglion neuron | syndromic congenital deafness | tyrosine kinase

About 30% of the 120 million people worldwide who suffer from congenital (early-onset) hearing loss are syndromic, and the remaining 70% are nonsyndromic (1–3). To elucidate the etiologies for the hearing losses, inner ears have been morphologically investigated as one of the target tissues. The inner ears contain the organ of Corti and the stria vascularis. The stria vascularis serves to maintain the endolymph potential. The organ of Corti, which consists of two kinds of sensory cells (inner hair cells and outer hair cells) is responsible for mechanotransduction, by which sound impulses are converted into neural impulses. Auditory information from the sensory cells is transmitted to spiral ganglion neurons (SGNs) as the primary carrier, followed by eventual transmission to the auditory cortex (1, 2). Most of the recent studies on hearing have focused on the expression level of a target molecule rather than activities in inner ears (1, 2). Thus, there have been very few studies aimed at determining whether activities of a target molecule cause hearing losses.

The c-*RET* protooncogene encodes a receptor tyrosine kinase, and glial cell-derived neurotrophic factor (GDNF) is one of the ligands for c-RET (4). The GDNF exerts its effect on target cells by binding to a GPI-anchored cell surface protein (GFRα1), which, in turn, recruits the receptor tyrosine kinase c-RET to form a multiple-subunit signaling complex. Formation of this complex results in c-RET autophosphorylation and a cascade of intracellular signaling to control cell survival (4–7).

Tyrosine 1062 (Y1062) in c-Ret is one of the most important autophosphorylation sites for its kinase activation and is a multidocking site for several signaling molecules, including SHC, a transmitter for c-Ret signaling (8–10). c-*RET* has been shown to be essential for the development and maintenance of the enteric nervous system (ENS) in both mice and humans (8, 9) and to be the most frequent causal gene of Hirschsprung disease (HSCR) in humans (20–25% of cases) (11, 12). In fact, severe HSCR with total intestinal aganglionosis has been shown to develop in homozygous knockin (KI) mice, in which Y1062 in c-Ret was replaced with phenylalanine (c-Ret-KI$^{Y1062F/Y1062F}$ mice) (6).

HSCR, which affects 1 in 5,000 births, is a congenital disorder of the ENS, and most cases are thought to be multigenic and multifactorial. A significantly increased risk for dominant sensorineural deafness in patients who have HSCR caused by *endothelin receptor type B* (*EDNRB*) (13) and *SOX10* (14) has been reported (11, 12). Despite the fact that c-*RET* is one of the responsible genes for HSCR, there is no direct evidence to link c-*Ret* and c-*RET* with deafness in mice and humans, presumably because of the short life span [postnatal day (P) 1–2)] of c-*Ret* homozygously deleted mice (15) to measure hearing levels.

In this study, we used c-Ret-KI$^{Y1062F/Y1062F}$ mice, which survive for 3–4 wk, and we focused on whether phosphorylation of c-Ret is relevant to hearing levels. Our results demonstrated that impairment of c-Ret phosphorylation causes syndromic congenital hearing loss with neurodegeneration of SGNs in c-Ret-KI$^{Y1062F/Y1062F}$ mice.

Results

Phosphorylation of c-Ret Y1062 in SGNs Increases in the Process of Hearing Development. We first examined the numbers of c-Ret protein expressed and Y1062-phosphorylated cells in inner ears from WT mice during the developmental stage of hearing after birth (Fig. 1). We found that c-Ret protein and phosphorylated Y1062 were clearly detectable in SGNs from WT mice on P14 (Fig. 1*A* and *B*, arrows). c-Ret protein was constantly expressed in SGNs throughout the hearing developmental stage after birth (P1–18) (Fig. 1*C*, *Left*), whereas the number of Y1062-phosphorylated SGNs was greatly increased in SGNs around P6–7, several days before the WT mice acquire intact hearing levels (around P12) [Fig. 1 *C Right* and *D*). Other areas (e.g., inner and outer hair cells, stria vascularis) of inner ears showed phosphorylated Y1062 in c-Ret (Fig. 1 *A* and *B*, arrowheads), but morphological abnormalities in inner and outer hair cells and the stria vascularis in c-Ret KI$^{Y1062F/Y1062F}$ mice were hardly detected (Figs. S1 and S2). SGNs have been reported to play an essential role in hearing by transmitting auditory information from sensory cells of the cochlea

Author contributions: N.O. and M.K. designed research; N.O., M.I.-E., T.S., and N.S. performed research; M.S., T.N., K.T., T.H., M.Y., G.S., M.J., N.A., A.H., and M.T. contributed new reagents/analytic tools; N.O., T.S., N.S., A.S., T.T., M.T., and M.K. analyzed data; and N.O. and M.K. wrote the paper.

The authors declare no conflict of interest.

This article is a PNAS Direct Submission.

[1]To whom correspondence should be addressed. E-mail: katomasa@isc.chubu.ac.jp.

This article contains supporting information online at www.pnas.org/lookup/suppl/doi:10.1073/pnas.1004520107/-/DCSupplemental.

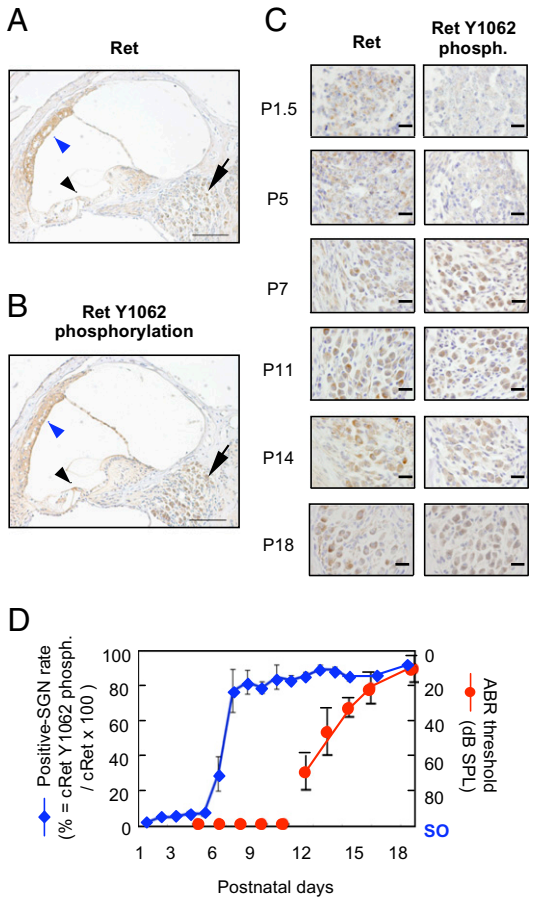

Fig. 1. Increased c-Ret Y1062-phosphorylated SGNs in the process of hearing development in WT mice. Immunohistochemical analyses of c-Ret protein–expressing cells (*A*) and Y1062-phosphorylated cells (*B*) in inner ears from 14-d-old WT mice (C57BL/6). c-Ret protein–expressing (*A*) and Y1062-phosphorylated (*B*) cells were detected in SGNs, acoustic neurons, and the stria vascularis in the inner ear from WT mice. Arrows in *A* and *B* indicate SGNs. Black arrowhead and blue arrowhead in *A* and *B* indicate inner and outer hair cells and stria vascularis, respectively. (*C*) Immunohistochemical analyses for serial sections of c-Ret–expressing (*Left*) and Y1062-phosphorylated (phosph., *Right*) SGNs from WT mice until P18. (Scale bars: *A* and *B*, 100 μm; *C*, 20 μm.) (*D*) Percentage (mean ± SE) of Y1062-phosphorylated SGNs from WT mice during the process of hearing development after birth. The *x* axis indicates days after birth of WT mice. The *y* axis for the blue line (mean ± SE; $n = 3$) indicates the percentage of Y1062-phosphorylated SGNs. The *y* axis for the red line (mean ± SE; $n = 5$) indicates hearing levels of WT mice measured by ABR. The effective measurement range of the ABR system is up to 90- to 100-dB SPL. Scale out (SO) indicates no ABR responses for 90- to 100-dB SPL. The method for staining and estimating the percentage is described in detail in *Materials and Methods*.

to the central nervous system (16). Therefore, we focused on the physiological roles in hearing level of phosphorylation of Y1062 in c-Ret tyrosine kinase in SGNs.

Congenital Deafness in c-Ret-KI$^{Y1062F/Y1062F}$ Mice. We next investigated tone burst-evoked auditory brainstem response (ABR) in c-Ret-KI$^{Y1062F/Y1062F}$ mice (6) to determine whether completely impaired phosphorylation of Y1062 in c-Ret kinase affects hearing levels. Thresholds for sound at 4–40 kHz in 18-d-old c-Ret-KI$^{Y1062F/Y1062F}$ mice [78- to 85-dB sound pressure level (SPL)] were much higher than those in littermate WT mice (20- to 55-dB SPL) (Fig. 2*A*). Latencies of all four ABR waves in c-Ret-KI$^{Y1062F/Y1062F}$ mice were also prolonged (Fig. 2*B*). These results suggest that c-Ret-KI$^{Y1062F/Y1062F}$ mice suffer from severe congenital deafness. On the other hand, hearing levels in other KI mice, in which serine 697 (S697, a putative protein kinase A phosphorylation site) in c-Ret was replaced with alanine (c-Ret-KI$^{S697A/S697A}$ mice), resulting in a mild HSCR phenotype (lack of the ENS limited to the distal colon) (17), were comparable to those in littermate WT mice (Fig. S3). These results demonstrate that early-onset syndromic deafness develops in c-Ret-KI$^{Y1062F/Y1062F}$ mice with severe HSCR (6) but not in c-Ret-KI$^{S697A/S697A}$ mice with mild HSCR (17).

Neurodegeneration of SGNs in c-Ret-KI$^{Y1062F/Y1062F}$ Mice. We next performed morphological analyses of Y1062-mediated congenital deafness. The number of c-Ret protein–expressed SGNs in c-Ret-KI$^{Y1062F/Y1062F}$ mice and that in littermate WT mice were no different on P14 (Fig. 3*A Upper*). The number of Y1062-phosphorylated SGNs was undetectably small in c-Ret-KI$^{Y1062F/Y1062F}$ mice, even on P14, compared with that in WT mice on P14 (Fig. 3 *A Lower* and *B*). Cell density of SGNs in the basal turn in c-Ret-KI$^{Y1062F/Y1062F}$ mice on P8 and P14 was 20–35% lower than that in the basal turn in littermate WT mice (Fig. 3 *C Lower* and *D*), although those on P2.5 were comparable in c-Ret-KI$^{Y1062F/Y1062F}$ mice and littermate WT mice (Fig. 3 *C Upper* and *D*). We further

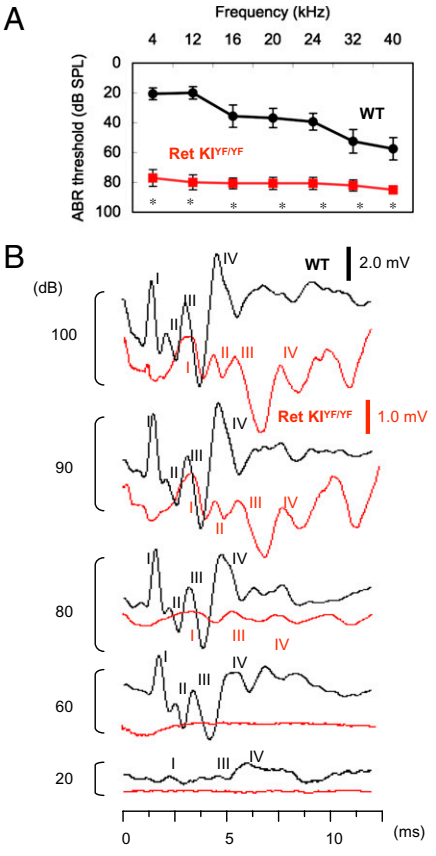

Fig. 2. Congenital deafness in c-Ret-KI$^{Y1062F/Y1062F}$ mice. (*A*) Hearing levels (mean ± SE) in 18-d-old c-Ret-KI$^{Y1062F/Y1062F}$ mice (Ret KI$^{YF/YF}$, red squares, $n = 8$) and littermate WT mice (WT, black circles, $n = 8$) measured by ABR. Significant difference (*$P < 0.01$) from the control was analyzed by the Mann–Whitney *U* test. (*B*) ABR waveforms of 18-d-old littermate WT mice (black line) and c-Ret-KI$^{YF/YF}$ mice (red line) at 20- to 100-dB SPL at 4 kHz are presented at different scales (WT, 2.0 mV; c-Ret-KI$^{YF/YF}$ mice, 1.0 mV) for clarity. The peaks of ABR waves I, II, III, and IV are indicated. The absolute latencies of all four ABR waves and the interpeak latencies for waves I–II (auditory nerve) at 100 dB were significantly increased in c-Ret-KI$^{YF/YF}$ mice as follows: wave I (WT: 1.52 ms vs. c-Ret-KI$^{YF/YF}$ mice: 3.18 ms), wave II (WT: 2.23 ms vs. c-Ret-KI$^{YF/YF}$ mice: 4.36 ms), wave III (WT: 3.24 ms vs. c-Ret-KI$^{YF/YF}$ mice: 5.58 ms), wave IV (WT: 4.86 ms vs. c-Ret-KI$^{YF/YF}$ mice: 7.43 ms), and waves I–II (WT: 0.82 ms vs. c-Ret-KI$^{YF/YF}$ mice: 1.21 ms).

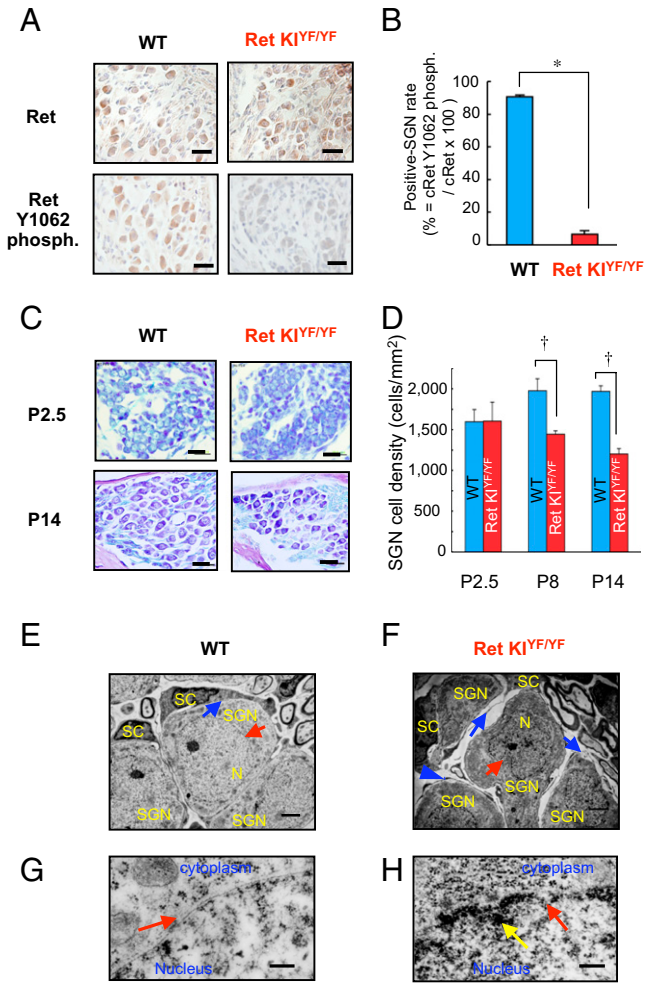

Fig. 3. Neurodegeneration of SGNs in c-Ret-KI$^{Y1062F/Y1062F}$ mice. (*A*) Immunohistochemical analyses for serial sections of the levels of c-Ret expression (*Upper*) and its phosphorylated Y1062 (*Lower*) in SGNs from 14-d-old littermate WT mice (WT, *Left*) and c-Ret-KI$^{Y1062F/Y1062F}$ mice (Ret KI$^{YF/YF}$, *Right*). (*B*) Percentage (mean ± SE) of Y1062-phosphorylated (phosph.) SGNs from 14-d-old c-Ret-KI$^{Y1062F/Y1062F}$ mice (Ret KI$^{YF/YF}$, red bar, $n = 3$) and littermate WT mice (WT, blue bar, $n = 3$). (Scale bars: 20 μm.) (*C*) Morphological analysis of SGNs from 2.5-d-old (*Upper*) and 14-d-old (*Lower*) WT mice (WT, *Left*) and littermate c-Ret-KI$^{Y1062F/Y1062F}$ mice (Ret KI$^{YF/YF}$, *Right*) by Kluver–Barrera staining. (*D*) Cell density (mean ± SE) of SGNs from 2.5-d-old (P2.5), 8-d-old (P8), and 14-d-old (P14) c-Ret-KI$^{Y1062F/Y1062F}$ mice (Ret KI$^{YF/YF}$, red bar, $n = 3$) and littermate WT mice (WT, blue bar, $n = 3$). (Scale bars: 20 μm.) The method for staining and estimating the percentage and cell density is described in detail in *Materials and Methods*. Significant difference ($^*P < 0.01$; $^\dagger P < 0.05$) from the control was analyzed by the Mann–Whitney *U* test (*B* and *D*). (*E–H*) TEM for SGNs from 14-d-old c-Ret-KI$^{Y1062F/Y1062F}$ mice (Ret KI$^{YF/YF}$, *F* and *H*) and littermate WT mice (WT, *E* and *G*). (*E* and *F*) Gap areas (blue arrows in *F*) between SGNs (SGN in *F*) with shrunken nuclei (red arrow in *F*) and Schwann cells (SC in *F*) were observed in c-Ret-KI$^{Y1062F/Y1062F}$ mice but not in littermate WT mice (blue arrow in *E*). N, nucleus. (*G* and *H*) Shrunken nuclei of SGNs with discontinuous nuclear membrane (red arrow in *H*) from c-Ret KI$^{Y1062F/Y1062F}$ mice and intact nuclear membrane of SGNs from WT mice (red arrow in *E* and *G*). The yellow arrow in *H* indicates condensed heterochromatin in the peripheral area of the nucleus of SGNs from c-Ret KI$^{Y1062F/Y1062F}$ mice. (Scale bars: *E* and *F*, 2 μm; *G* and *H*, 500 nm.)

performed detailed morphological analyses of SGNs from c-Ret-KI$^{Y1062F/Y1062F}$ mice during the hearing developmental stage by transmission electron microscopy (TEM) (Fig. 3 *E–H*). SGNs in c-Ret-KI$^{Y1062F/Y1062F}$ mice on P14 exhibited shrunken nuclei (Fig. 3*F*, red arrow) with discontinuous nuclear membranes (Fig. 3*H*, red arrow) and highly condensed heterochromatin in the peripheral area (Fig. 3*H*, yellow arrow), whereas those in littermate WT mice had intact bilayer membranes of nuclei (Fig. 3 *E* and *G*, red arrows). c-Ret-KI$^{Y1062F/Y1062F}$ mice on P14 also showed gaps between SGNs and Schwann cells (Fig. 3*F*, blue arrows) compared with those in littermate WT mice (Fig. 3*E*, blue arrow). On the other hand, no hallmarks for apoptotic signals in SGNs were found in either c-Ret-KI$^{Y1062F/Y1062F}$ mice or littermate WT mice on P8, P12, and P14 (Fig. S4).

Congenital Hearing Loss in c-Ret-KI$^{Y1062F/Y1062F}$ Mice Was Rescued by Introducing Constitutively Activated RET. We then tried to rescue the congenital hearing loss in c-Ret-KI$^{Y1062F/Y1062F}$ mice. For this purpose, we crossed c-Ret-KI$^{Y1062F/Y1062F}$ mice with constitutively activated RET (RFP-RET)-carrying transgenic mice (RET-Tg mice) of line 242 (18) and established c-Ret-KI$^{Y1062F/Y1062F}$;RET-Tg mice. Congenital hearing loss was again observed in 21-d-old c-Ret-KI$^{Y1062F/Y1062F}$ mice (Fig. 4*A*, red squares, and Fig. S5*B*). Hearing levels in c-Ret-KI$^{Y1062F/Y1062F}$;RET-Tg mice were comparable to those in littermate WT mice and were significantly improved compared with those in littermate c-Ret-KI$^{Y1062F/Y1062F}$ mice (Fig. 4*A* and Fig. S5). Correspondingly, the number of Y1062-phosphorylated SGNs in c-Ret–expressed SGNs and cell density of SGNs from c-Ret-KI$^{Y1062F/Y1062F}$;RET-Tg mice were comparable to those from littermate WT mice and significantly higher than those from c-Ret-KI$^{Y1062F/Y1062F}$ mice (Fig. 4 *B–E*). On the other hand, results of a previous study in vitro (19) and our results (Fig. S6) suggested that phosphorylated levels of Y1062 in c-RET modulate NF-κB activities via AKT phosphorylation levels in neural cells. In addition, impairments of NF-κB–mediating signaling have been shown to cause down-regulation of calbindin D28k, which contributes to neuronal survival, leading to neurodegenerative disorders (20). Our results and the results of previous studies mentioned above encouraged us to determine immunohistochemically the phosphorylation levels of NF-κB and Akt and the expression levels of calbindin D28k in SGNs from c-Ret-KI$^{Y1062F/Y1062F}$ mice to analyze the etiology of c-Ret–mediated congenital hearing loss further. Results of this study in vivo showed that not only phosphorylation levels of NF-κB and Akt but expression levels of calbindin D28k were impaired in SGNs from c-Ret-KI$^{Y1062F/Y1062F}$ mice and were restored in SGNs from c-Ret-KI$^{Y1062F/Y1062F}$;RET-Tg mice (Fig. 5).

Discussion

In this study, we provide direct evidence that c-*Ret* is a congenital deafness-related molecule in mice. Our results partially correspond to results of previous studies showing that GDNF has a protective effect on antibiotics-induced ototoxicities (21–24). Mutation of c-Ret at Y1062 has been shown to fail to respond to GDNF in vitro (19). However, previous studies have indicated that there is a Ret-independent signaling pathway stimulated by GDNF (5, 8, 25). Moreover, it has not been determined whether impairment of c-Ret kinase activity affects hearing, even though it has been shown that c-Ret, GFRα1, and GDNF are expressed in auditory neurons (26, 27). Our results strongly suggest that impaired phosphorylation of Y1062 in c-Ret without change in the expression level results in the development of congenital hearing loss with neurodegeneration of SGNs in mice. We further demonstrated congenital hearing loss in human patients with c-*RET*–mediated HSCR. Thus, this study indicated the importance of considering the activity as well as the expression of the target molecule to elucidate the etiologies of hereditary deafness.

This study demonstrated that c-Ret-KI$^{Y1062F/Y1062F}$ mice had severe congenital deafness with neurodegeneration of SGNs, resulting in decreased numbers of SGNs on P8–18 (Figs. 2 and 3). In contrast, the number and morphology of SGNs were comparable between c-Ret-KI$^{Y1062F/Y1062F}$ mice and WT mice on P2–3 (Fig. 3 *C* and *D*). These results suggest that SGNs even from c-Ret-KI$^{Y1062F/Y1062F}$ mice developed normally at least until P3, when

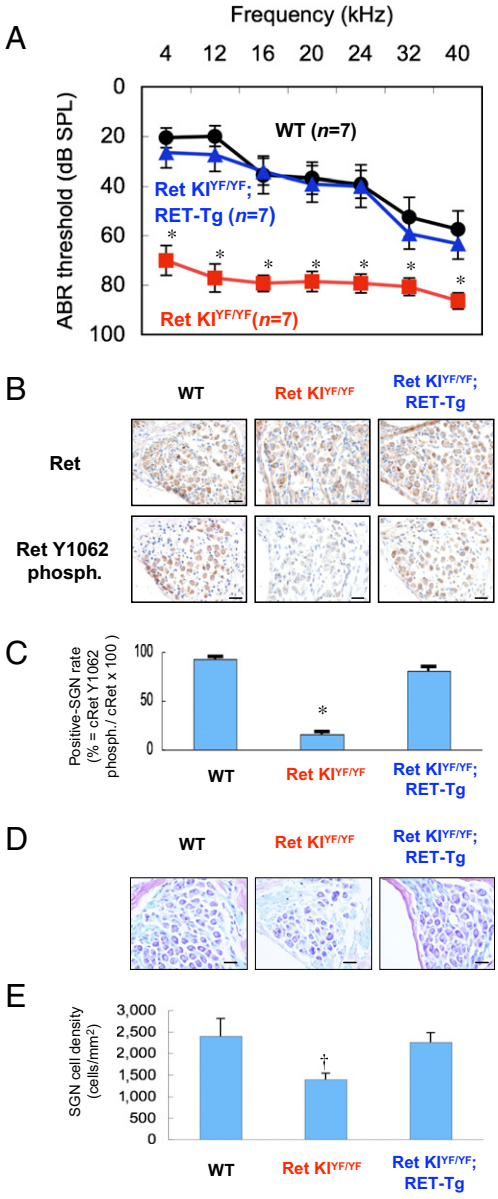

Fig. 4. Rescue of congenital hearing loss in c-Ret-KI$^{Y1062F/Y1062F}$ mice by introducing constitutively activated RET. (*A*) Hearing levels (mean ± SE) in 21-d-old WT mice (WT, black circles, $n = 7$), littermate c-Ret-KI$^{Y1062F/Y1062F}$ mice (Ret KI$^{YF/YF}$, red squares, $n = 7$), and c-Ret-KI$^{Y1062F/Y1062F}$;RFP/RET mice (Ret KI$^{YF/YF}$; RET-Tg, blue triangles, $n = 7$) mice measured by ABR. (*B*) Immunohistochemical analyses for serial sections of the levels of c-Ret expression (*Upper*) and its phosphorylated (phosph.) Y1062 (*Lower*) in SGNs from 15-d-old mice of three different strains (WT, Ret KI$^{YF/YF}$, and Ret KI$^{YF/YF}$;RET-Tg). (Scale bars: 20 μm.) (*C*) Percentages (mean ± SE) of Y1062-phosphorylated SGNs from littermate 15-d-old mice of three different strains (WT, Ret KI$^{YF/YF}$, and Ret KI$^{YF/YF}$;RET-Tg) are presented. (*D*) Morphological analysis of SGNs from 15-d-old mice of three different strains (WT, Ret KI$^{YF/YF}$, and Ret KI$^{YF/YF}$;RET-Tg) with Kluver–Barrera staining. (Scale bars: 20 μm.) (*E*) Cell density (mean ± SE) of SGNs from three mice of each mouse strain is presented. The method for staining and estimating the percentage and the cell density is described in detail in *Materials and Methods*. Significant difference (*$P < 0.01$; †$P < 0.05$) from the control was analyzed by the Kruskal–Wallis *H* test (*A, C, and E*).

Y1062 phosphorylation in c-Ret of SGNs from WT mice was undetectable, but those from c-Ret-KI$^{Y1062F/Y1062F}$ mice no longer survived on P8–18, when the level of Y1062 phosphorylation in c-Ret of SGNs from WT mice was high (summarized in Fig. S7 *A–C*). Y1062 phosphorylation in c-Ret has been reported to mediate

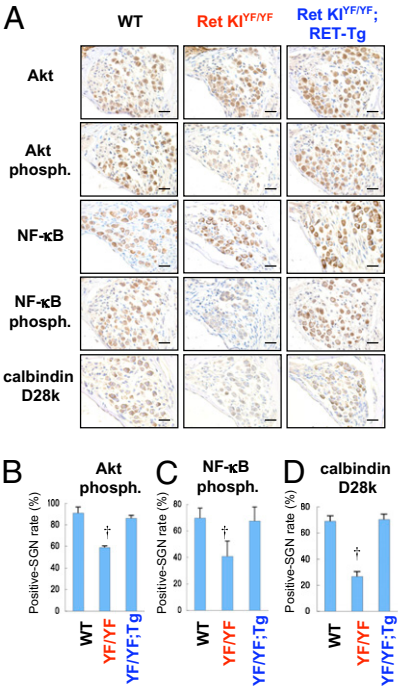

Fig. 5. Immunohistochemical analyses of phosphorylation levels of NF-κB and Akt and expression levels of calbindin D28k in SGNs from c-Ret-KI$^{Y1062F/Y1062F}$ mice. (*A*) Immunohistochemical analyses of SGNs from 15-d-old WT mice, littermate c-Ret-KI$^{Y1062F/Y1062F}$ mice (Ret KI$^{YF/YF}$) and c-Ret-KI$^{Y1062F/Y1062F}$;RFP/RET mice (Ret KI$^{YF/YF}$;RET-Tg) with polyclonal antibodies against Akt, phosphorylated Akt (Akt phosph.), NF-κB, phosphorylated NF-κB (NF-κB phosph.), and calbindin D28k. All specimens were developed with diaminobenzidine, followed by counterstaining with hematoxylin. (Scale bars: 20 μm.) (*B–D*) Percentage of positive SGN number (mean ± SE) of phosphorylated Akt (*B*), phosphorylated NF-κB (*C*), and calbindin D28k (*D*) in WT mice, littermate c-Ret-KI$^{Y1062F/Y1062F}$ mice (YF/YF), and c-Ret-KI$^{Y1062F/Y1062F}$;RFP/RET mice (YF/YF;RET-Tg) is presented. The method for estimating the percentage is described in detail in *Materials and Methods*. Significant difference (†$P < 0.05$) from the control was analyzed by the Kruskal–Wallis *H* test in *B–D*.

several biological responses, including survival of neuronal cells (8, 19). We therefore conclude that complete impairment of Y1062 phosphorylation in c-Ret affects survival of SGNs during the late stage of hearing development after birth in mice (around P8–18).

Our results further demonstrated that c-Ret–mediated congenital hearing loss involves impaired activities of Akt and NF-κB, with impaired expression of calbindin D28k in SGNs (Fig. 5). The impairments of these molecules in SGNs from c-Ret-KI$^{Y1062F/Y1062F}$ mice were clearly rescued by introducing constitutively activated RET (Fig. 5). These results partially correspond to results of a previous study in vitro and in vivo showing that GDNF induces expression of calbindin D28k, which promotes neural survival, via Akt/NF-κB signaling in substantia nigra neurons (28). Thus, our results suggest a mechanistic model for c-Ret–mediated congenital deafness in which impairments of the c-Ret–mediated signaling pathway cause decreased expression of calbindin D28k via Akt/NF-κB signaling, resulting in auditory nerve degeneration (summarized in Fig. S7 *D* and *E*). The neurodegeneration of SGNs from c-Ret-KI$^{Y1062F/Y1062F}$ mice did not involve the hallmark of apoptotic signals (Fig. S4). The results of a previous study also showed that neurodegeneration of postmigratory enteric neurons did not involve apoptotic signals during the developmental stage in mice with conditional ablation of c-*Ret* (29).

Hearing losses in three patients with HSCR were previously reported (30). Because the causal genes in patients who have HSCR have not been identified, we performed mutational anal-

ysis in this study for *RET*, *GDNF*, *neurturin* (*NTN*), *SOX10*, *EDNRB*, and *endothelin 3* (*ET-3*) genes of patients with HSCR, as listed in Table S1. We found that the patients with HSCR who have hearing losses have mutations only in RET among the above genes (Fig. S8 and Table S1). The results obtained with c-*Ret* KI mice demonstrate that impairments of Y1062 phosphorylation in c-Ret cause congenital hearing loss (Fig. 2 and 4), whereas normal hearing is maintained with even complete impairment of S697 phosphorylation in c-Ret (Fig. S3). In humans, we found hearing impairments in three patients with severe HSCR, including two male patients with homozygous and heterozygous mutations at arginine 969 located in c-RET kinase domains and one male patient with a nucleotide deletion at *RET* codon 13, resulting in a frameshift and termination at codon 22. No hearing impairments were found in patients with other heterozygous missense mutations at codons 30, 144, 489, 734, 897, and 942 (Table S1). Therefore, these results suggest that impairments of c-*Ret* and c-*RET* cause hearing losses in mice and humans in a site-dependent manner. Further study is needed to determine the correlation between mutational sites of c-*Ret* and c-*RET* and hearing losses in mice and humans.

We finally demonstrated that congenital hearing loss involving neurodegeneration of SGNs in c-Ret-KI$^{Y1062F/Y1062F}$ mice was rescued by introducing constitutively activated RET (Figs. 4 and 5). Despite a significantly increased risk for syndromic deafness in patients with HSCR (11, 12), no effective therapies for deafness have been established. Therefore, our findings will be useful for the development of therapeutical strategies targeting c-RET kinase against hearing impairments.

Materials and Methods

Mice. c-Ret-KI$^{Y1062F/Y1062F}$ mice (6), c-Ret-KI$^{S697A/S697A}$ mice (17), and RET-Tg mice of line 242 (18) were previously reported. There are no reports about hearing levels in these strains except a previous report showing that hearing levels in 10-wk-old RET-Tg mice and littermate WT mice were comparable (31). In this study, c-Ret-KI$^{Y1062F/+}$;RET-Tg mice were newly established by crossing the c-Ret-KI$^{Y1062F/+}$ mouse with the RET-Tg mouse. All experiments were authorized by the Institutional Animal Care and Use Committee of Chubu University (approval no. 2210038) and the Institutional Recombinant DNA Experiment Committee of Chubu University (approval no. 06-01) and followed the Japanese Government Regulations for Animal Experiments.

Measurement of Hearing. ABR measurements (AD Instruments Pty. Ltd.) were performed as described previously (30, 32). Tone burst stimuli were measured at 5 dB stepwise from 0-dB SPL to 70- or 90-dB SPL. The threshold was obtained by identifying the lowest level of I wave of ABR recognized. Data are presented as mean ± SE.

Morphological Analysis with a Light Microscope. After perfusion fixation with Bouin's solution, cochleae from 0.5- to 21-d-old mice were immersed in the same solution overnight and for 1 wk, respectively. Kluver–Barrera staining was performed with paraffin sections. Immunohistochemical analyses with polyclonal antibodies against c-Ret protein (1:150; Immuno Biological Laboratories), phosphorylated c-Ret Y1062 (1:150) (33), Akt (1:300; Cell Signaling), phosphorylated Akt (1:50; Cell Signaling), and phosphorylated NF-κB p50 (1:50; Santa Cruz) were performed on frozen sections with Can Get Signal immunostaining solution (TOYOBO). Immunohistochemical analysis with polyclonal antibodies against NF-κB p50 (1:100; Santa Cruz) and calbindin D28k (1:150; Chemicon) was performed for paraffin sections. For the detection of NF-κB p50, the paraffin sections were treated with 10 mM sodium citrate (pH 6.0) for 10 min at 90 °C for antigen retrieval. For the detection of calbindin D28k, the paraffin sections were treated with 10 mM sodium citrate (pH 6.0) for 10 min at 90 °C for antigen retrieval, and Can Get Signal immunostaining solution was used as dilution buffer. The VECTASTAIN ABC kit (Vector) and Envision kit/HRP (diaminobenzidine; DAKO) were used in each immunohistochemical analysis with counterstained hematoxylin. Immunohistochemical estimation of the percentage of positive SGNs detected by antibodies was calculated using the software program WinROOF (Mitani Corp.), as previously reported (34). In brief, the number of immunohistochemically positive SGNs was divided by the total number of SGNs in each Rosenthal's canal from three or four mice for each mouse strain. In total, 160–200 SGNs were counted for each evaluation of cell density and percentage. In the case of immunohistochemical estimation of phosphorylated protein, percentage (mean ± SE) was calculated by dividing the number of phosphorylated SGNs by the number of the protein-expressing SGNs in each Rosenthal's canal from three or four mice for each mouse strain. Estimation of the cell density of SGNs with Kluver–Barrera staining basically followed the previous method (35, 36). In brief, the area of Rosenthal's canal in five sections from each mouse was measured with the software program WinROOF. The cell density of SGNs from three or four mice for each mouse strain was calculated by dividing the cell number of SGNs in the measured Rosenthal's canal by the area. In total, 160–200 SGNs in five sections from each mouse were examined. In total, 160–200 SGNs were counted for each evaluation of cell density and percentage.

Morphological Analysis by TEM. Preparation of tissues for TEM basically followed the previous method (35). In brief, after perfusion fixation with a fixative solution I containing 2% (vol/vol) paraformaldehyde, 2% (vol/vol) glutaraldehyde and 0.3 M Hepes (pH 7.4), dissected murine cochleae were immersed in the same fixative solution overnight at 4 °C. The cochleae were then fixed with a fixative solution II containing 2% (vol/vol) osmium tetroxide and 0.3 M Hepes (pH 7.4) at 4 °C for 3 h. After rinsing off the fixative solution, the cochleae were dehydrated with a graded series of ethanol and embedded in epoxy resin (Quetol 651; Nisshin EM). Ultrathin sections (thickness = 70 nm) were observed under an electron microscope at 80 kV (JEM1200EX; JEOL).

Mutational Analysis in Patients with HSCR. We analyzed mutations of *RET*, *GDNF*, *NTN*, *SOX10*, *EDNRB*, and *ET-3* genes in DNA samples from 15 children with total colonic aganglionosis, as described previously (37). Amplification was accomplished with a reaction mixture containing 100 ng of lymphocyte DNA, 2.5 μM each set of primers, 200 μM dNTP, 10 mM Tris HCl (pH 8.3), 1.5 mM $MgCl_2$, 50 mM KCl, and 1.0 U of Taq DNA polymerase. Thermocycling conditions consisted of denaturation at 95 °C for 9 min, 45 cycles of annealing at 60 °C for 2 min, and extension at 95 °C for 30 s, followed by a denaturing step at 60 °C for 3 min in an automatic thermocycler (GeneAmp PCR System 2400; Perkin–Elmer). The DNA sequencings were carried out by the direct dyedeoxy terminator cycle method using a fluorescent automatic DNA sequencer (Model 373A DNA Sequencing systems; Applied Biosystems).

Ethical Considerations. The study was approved by the Ethics Committee of Chubu University (approval no. 20008-4) and conducted according to the Declaration of Helsinki. All patients gave voluntary written informed consent.

Statistics. Significant difference ($^*P < 0.01$; $^\dagger P < 0.05$) from the control was analyzed by the Mann–Whitney *U* test (Figs. 2 and 3) and the Kruskal–Wallis *H* test (Figs. 4 and 5).

ACKNOWLEDGMENTS. We thank Kyoko Ohgami, Yoko Kato, Yukie Ohtsuka, and Harumi Ohno for their technical assistance. We also thank Dr. Izumi Nakashima and the laboratory members for their helpful discussions. This study was supported in part by Grants-in-Aid for Scientific Research (B) Grants 19390168 and 20406003 (to M.K.) and Grants-in-Aid for Young Scientists (B) Grant 18790738 (to N.O.) and Grant 20791232 (to M.I.-E.) from the Ministry of Education, Culture, Sports, Science, and Technology; the COE Project for Private Universities (Grant S0801055) from the Ministry of Education, Culture, Sports, Science, and Technology; the Uehara Memorial Foundation (M.K.), Rohto Awards (M.K.), Chubu University Grants A (to N.O. and M. K.), B (to N.O.), and C (to M.K.); and the GCOE Project from the Ministry of Education, Culture, Sports, Science, and Technology (to M.T.).

1. Lalwani AK, Gürtler N (2008) Sensorineural hearing loss, the aging inner ear, and hereditary hearing impairment. *CURRENT Diagnosis and Treatment in Otolaryngology—Head and Neck Surgery*, ed Lalwani AK (McGraw–Hill, New York), 2nd Ed, pp 683–704.
2. Brown SD, Hardisty-Hughes RE, Mburu P (2008) Quiet as a mouse: Dissecting the molecular and genetic basis of hearing. *Nat Rev Genet* 9:277–290.
3. Gratton MA, Vázquez AE (2003) Age-related hearing loss: Current research. *Curr Opin Otolaryngol Head Neck Surg* 11:367–371.
4. Takahashi M (2001) The GDNF/RET signaling pathway and human diseases. *Cytokine Growth Factor Rev* 12:361–373.
5. Trupp M, Scott R, Whittemore SR, Ibáñez CF (1999) Ret-dependent and -independent mechanisms of glial cell line-derived neurotrophic factor signaling in neuronal cells. *J Biol Chem* 274:20885–20894.
6. Jijiwa M, et al. (2004) A targeting mutation of tyrosine 1062 in Ret causes a marked decrease of enteric neurons and renal hypoplasia. *Mol Cell Biol* 24:8026–8036.

7. Drosten M, Pützer BM (2006) Mechanisms of Disease: Cancer targeting and the impact of oncogenic RET for medullary thyroid carcinoma therapy. *Nat Clin Pract Oncol* 3: 564–574.
8. Airaksinen MS, Saarma M (2002) The GDNF family: Signaling, biological functions and therapeutic value. *Nat Rev Neurosci* 3:383–394.
9. Heanue TA, Pachnis V (2007) Enteric nervous system development and Hirschsprung's disease: Advances in genetic and stem cell studies. *Nat Rev Neurosci* 8:466–479.
10. Kato M, et al. (2002) Repair by Src kinase of function-impaired RET with multiple endocrine neoplasia type 2A mutation with substitutions of tyrosines in the COOH-terminal kinase domain for phenylalanine. *Cancer Res* 62:2414–2422.
11. Moore SW, Johnson AG (1998) Hirschsprung's disease: Genetic and functional associations of Down's and Waardenburg syndromes. *Semin Pediatr Surg* 7:156–161.
12. Moore SW (2006) The contribution of associated congenital anomalies in understanding Hirschsprung's disease. *Pediatr Surg Int* 22:305–315.
13. Attié T, et al. (1995) Mutation of the endothelin-receptor B gene in Waardenburg-Hirschsprung disease. *Hum Mol Genet* 4:2407–2409.
14. Pingault V, et al. (1998) SOX10 mutations in patients with Waardenburg-Hirschsprung disease. *Nat Genet* 18:171–173.
15. Schuchardt A, D'Agati V, Larsson-Blomberg L, Costantini F, Pachnis V (1994) Defects in the kidney and enteric nervous system of mice lacking the tyrosine kinase receptor Ret. *Nature* 367:380–383.
16. Rubel EW, Fritzsch B (2002) Auditory system development: Primary auditory neurons and their targets. *Annu Rev Neurosci* 25:51–101.
17. Asai N, et al. (2006) Targeted mutation of serine 697 in the Ret tyrosine kinase causes migration defect of enteric neural crest cells. *Development* 133:4507–4516.
18. Kato M, et al. (1999) Linkage between melanocytic tumor development and early burst of Ret protein expression for tolerance induction in metallothionein-I/ret transgenic mouse lines. *Oncogene* 18:837–842.
19. Hayashi H, et al. (2000) Characterization of intracellular signals via tyrosine 1062 in RET activated by glial cell line-derived neurotrophic factor. *Oncogene* 19:4469–4475.
20. Mattson MP, Camandola S (2001) NF-kappaB in neuronal plasticity and neurodegenerative disorders. *J Clin Invest* 107:247–254.
21. Suzuki M, et al. (2000) Effect of transgenic GDNF expression on gentamicin-induced cochlear and vestibular toxicity. *Gene Ther* 7:1046–1054.
22. Yagi M, et al. (2000) Spiral ganglion neurons are protected from degeneration by GDNF gene therapy. *J Assoc Res Otolaryngol* 1:315–325.
23. Liu Y, et al. (2008) Protection against aminoglycoside-induced ototoxicity by regulated AAV vector-mediated GDNF gene transfer into the cochlea. *Mol Ther* 16: 474–480.
24. Scheper V, et al. (2009) Effects of delayed treatment with combined GDNF and continuous electrical stimulation on spiral ganglion cell survival in deafened guinea pigs. *J Neurosci Res* 87:1389–1399.
25. Poteryaev D, et al. (1999) GDNF triggers a novel ret-independent Src kinase family-coupled signaling via a GPI-linked GDNF receptor alpha1. *FEBS Lett* 463:63–66.
26. Stöver T, Gong TL, Cho Y, Altschuler RA, Lomax MI (2000) Expression of the GDNF family members and their receptors in the mature rat cochlea. *Brain Res Mol Brain Res* 76:25–35.
27. Stöver T, Nam Y, Gong TL, Lomax MI, Altschuler RA (2001) Glial cell line-derived neurotrophic factor (GDNF) and its receptor complex are expressed in the auditory nerve of the mature rat cochlea. *Hear Res* 155:143–151.
28. Wang HJ, et al. (2008) Calbindin-D28K expression induced by glial cell line-derived neurotrophic factor in substantia nigra neurons dependent on PI3K/Akt/NF-kappaB signaling pathway. *Eur J Pharmacol* 595:7–12.
29. Uesaka T, Nagashimada M, Yonemura S, Enomoto H (2008) Diminished Ret expression compromises neuronal survival in the colon and causes intestinal aganglionosis in mice. *J Clin Invest* 118:1890–1898.
30. Shimotake T, Iwai N (1994) Auditory brainstem response in children with total intestinal aganglionosis. *Lancet* 343:1362.
31. Hayashi H, et al. (2004) A novel RFP-RET transgenic mouse model with abundant eumelanin in the cochlea. *Hear Res* 195:35–40.
32. Zheng QY, Johnson KR, Erway LC (1999) Assessment of hearing in 80 inbred strains of mice by ABR threshold analyses. *Hear Res* 130:94–107.
33. Yamamoto M, et al. (2001) Preserved phosphorylation of RET receptor protein in spinal motor neurons of patients with amyotrophic lateral sclerosis: An immunohistochemical study by a phosphorylation-specific antibody at tyrosine 1062. *Brain Res* 912:89–94.
34. Enomoto A, et al. (2009) Roles of disrupted-in-schizophrenia 1-interacting protein girdin in postnatal development of the dentate gyrus. *Neuron* 63:774–787.
35. Lang H, et al. (2006) Nuclear factor kappaB deficiency is associated with auditory nerve degeneration and increased noise-induced hearing loss. *J Neurosci* 26:3541–3550.
36. Shimada A, Ohta A, Akiguchi I, Takeda T (1992) Inbred SAM-P/10 as a mouse model of spontaneous, inherited brain atrophy. *J Neuropathol Exp Neurol* 51:440–450.
37. Inoue K, Shimotake T, Iwai N (2000) Mutational analysis of RET/GDNF/NTN genes in children with total colonic aganglionosis with small bowel involvement. *Am J Med Genet* 93:278–284.